Visualization of aerodynamic flow fields using photorefractive crystals

A. Hafiz, R. Magnusson, J. S. Bagby, D. R. Wilson, and T. D. Black

Interferometry based on double exposure Fourier transform holography in photorefractive crystals is applied for visualization of aerodynamic flow fields. The interferograms obtained are of similar quality as those produced using holographic film but with greatly simplified procedures. The results presented are obtained using a high-power cw argon laser and iron doped lithium niobate crystals. The angular characteristics of the Fourier transform data holograms are studied.

I. Introduction

Holographic interferometry is an important diagnostic technique with a large number of practical applications. Global visualization of spatial refractive index distributions may be obtained using this technique. Example application areas include aerodynamics, plasma diagnostics, and heat transfer. Holographic interferometry allows the resultant refractive index distributions to be quantitatively evaluated in these cases without disturbing the flow.

To date, holographic film has been used as the recording medium in most of the holographic interferometry experiments reported in the literature. The use of film is basically undesirable due to the tedium involved in developing the exposed film and due to the necessity of a darkened work area. Self-developing or photorefractive optical crystals offer an alternative to the use of film in holographic interferometry. In this paper, interferometric visualization of aerodynamic flow fields using photorefractive crystals is reported.

Photorefractive crystals have many favorable characteristics for holographic interferometry. These include instantaneous hologram storage (no development needed), large information storage capacity via angular multiplexing, erasability and reusability, available hologram fixing techniques, wide hologram lifetime range, real time recording and readout, high sensitivity and resolution, controllable materials properties, and, at last, sensitivity to laser recording light only with no need to work in the dark. Hologram recording in such materials is based on the photorefractive effect.[1]

Only limited amount of research has been done on interferometry using photorefractive crystals as the storage medium. Magnusson *et al.*[2] reported initial experimental results in iron doped lithium niobate where a relatively low power laser was used requiring long exposures (~1 s). Real time, double exposure interferograms have been produced with bismuth silicon oxide (BSO) crystals.[3,4] These crystals are very sensitive at argon-ion laser wavelengths (in the blue and the green spectral region), requiring similar energy densities as silver halide photographic emulsions but also requiring the application of an external electric field. Due to this high sensitivity, retention time is very short and readout is destructive. Thus, while reading, the interferometric image should be stored, for example, via a vidicon tube for further processing. These workers have also presented results on time average holographic interferometry using this material.[5] Real time interferometry in four-wave mixing using bismuth germanium oxide (BGO) crystals has also been demonstrated.[6] In that experiment, a reflection type geometry was used without an external electric field yielding interferograms with a short lifetime (~1 s). BSO and BGO thus appear to be most useful in real time or near real time applications while volume hologram superpositions are not feasible in these crystals due to their high sensitivity.

This paper presents experimental work on aerodynamic flow field visualization using double exposure hologram recording in lithium niobate crystals doped with iron (Fe:$LiNbO_3$). In the current experiments, many objects are used and holograms produced with exposure times around 10–50 ms are presented. The

All authors are with University of Texas at Arlington, Arlington, Texas 76019; D. R. Wilson is in the Department of Aerospace Engineering, T. D. Black is in the Department of Physics, and the other authors are in the Department of Electrical Engineering.

Received 22 June 1988.
0003-6935/89/081521-04$02.00/0.

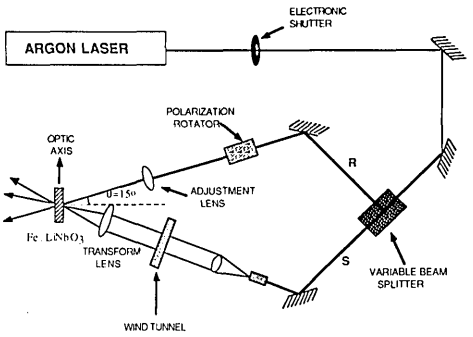

Fig. 1. Experimental system.

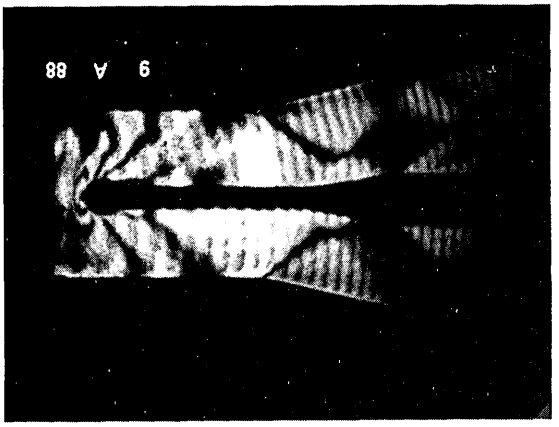

Fig. 2. Interferogram of the flow field in the wind tunnel. The object is circularly symmetric with a ball tip. The pressure is 220 psi.

results are greatly improved over those previously reported.[2] The different objects used in this work demonstrate the sensitivity of the flow to the target physical shape and the ability of the technique used to record these differences. It is also demonstrated that good sensitivity to varying flow conditions for a given object is obtained. Multiple storage of interferograms via angular multiplexing is demonstrated.

II. Experiments

The experimental system is shown in Fig. 1. A high power cw argon-ion laser with a single frequency line of 514.5-nm wavelength is used. The beam splitter divides the beam into an object beam and a reference beam. The object beam is collimated to a diameter of 50 mm. It passes through the wind tunnel window and then through a Fourier transform lens. The reference beam is slightly focused to a desired diameter using a long focal length converging lens to achieve optimum overlap of the two beams. A polarization rotator is placed in the reference beam to control the readout polarization of the stored holograms (s- or p-polarization readout). The two beams meet at a point 5 mm away from the focal plane of the Fourier transformed object wave. The external Bragg angle at that point is 15°. The 0.05% iron doped lithium niobate crystal is used in the transmission geometry configuration. It is of vital importance that the crystal optic axis is oriented orthogonal to the holographic fringes to take advantage of the photovoltaic effect and the attendant efficient charge transport. The two beams are s-polarized when recording the holograms. The crystal allows recording in various locations because its dimensions are significantly larger (10 × 10 × 1.6 mm) than the small size spot areas that are used for the holograms. The object beam has a cross sectional area of ~1 mm^2 (at the crystal) while the reference beam is ~3 mm^2 to make certain that full overlap is obtained. Typically, the power density used in these experiments is ~16 W/cm^2 for the two beams combined. Reference (R) to object (S) beam ratio is of the order of 3 (R/S ≅ 3).

The wind tunnel is driven by nitrogen gas and the flow fields for the objects of different sizes and shapes are recorded. The first interferogram is recorded under symmetric conditions (unslanted holograms) whereas the rest are written via angular multiplexing with ~0.1–1° angular spacing (achieved by crystal rotation) between the double exposure holograms. The experiment is performed in many different configurations. The holographic exposure is set to various values, typically 10–50 ms.

III. Results

The object mounted in the wind tunnel for the experiments reported here is circularly symmetric with a ball tip. The object wave thus traverses what is actually a 3-D flow structure. If the objects were constant along the laser beam direction (i.e., spanned across the wind tunnel), improved fringe contrast would be obtained. The wind tunnel window has dimensions of 10 × 20 mm.

An interferogram produced by the reconstruction of a double exposure hologram (first exposure, flow off; second exposure, flow on) is shown in Fig. 2. This demonstrates the visualization of the flow field created by this object. The shock waves generated by the object and bouncing off the tunnel walls are clearly shown. The input pressure used is 220 psi. Two 30-ms exposures are used. The total laser power is 16 W/cm^2. The superimposed fine line structure is due to multiple internal reflections between the crystal surfaces.

To demonstrate the sensitivity of this technique to variations in the aerodynamic conditions, additional visualizations are produced under varying flow pressure. Figure 3 is similar to Fig. 2 except that the input flow pressure is now 270 psi, with corresponding increased fringe density and higher bow-wave angle. Figure 4 is similar but at 320 psi. Note the shock waves bouncing off the tunnel walls.

A variety of test objects have been used during the course of this work under widely varying experimental conditions. The experimental results are easily and conveniently obtained. Sequential recording is accomplished using angular multiplexing of the double exposure holograms. For the data in Figs. 2–4, the interferograms are angularly multiplexed with the (external) angular separation $\Delta\theta' = 0.5°$. Each double exposure hologram is reconstructed on the Bragg angle. In Fig. 5 an example interferogram produced via

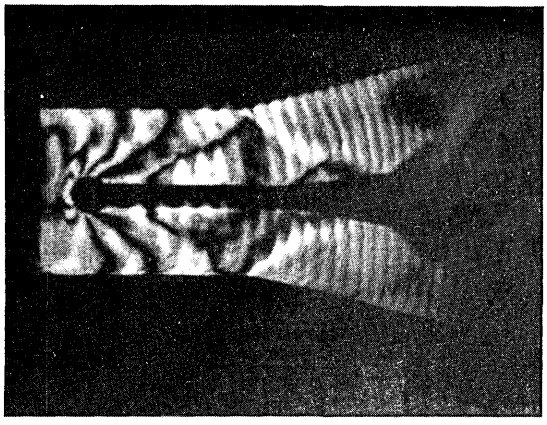

Fig. 3. Similar to Fig. 2 but with 270-psi pressure.

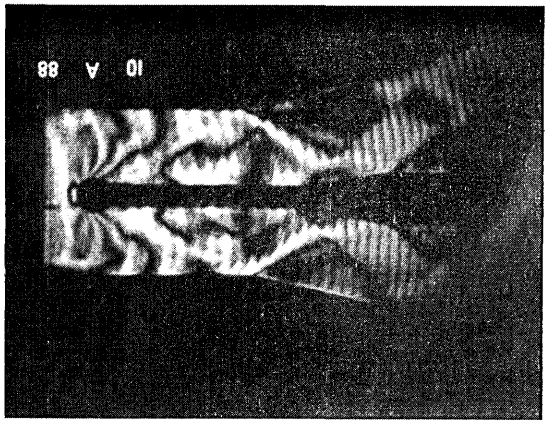

Fig. 4. Similar to Fig. 2 but at 320 psi.

angularly stacked holograms (in the same physical crystal location) is shown. The same object is used. This interferogram corresponds to the thirteenth in a set of double exposure holograms, all recrecorded under different conditions and with several different objects. Note that the quality of the interferogram has not substantially deteriorated over that of Figs. 2–4.

To further quantify the storage of multiple double exposure holograms via angular multiplexing, several sets of interferograms have been produced with the diffraction efficiency and angular selectivity of each such hologram measured. A curve of the diffraction efficiency vs the readout angle is presented in Fig. 6. In this collection of holograms, the change in the Bragg angle was $\Delta\theta' = 1.0°$. All the interferograms were recorded under the same conditions with two 30-ms exposures used for each. Typical diffraction efficiency for s-polarization readout is seen in this figure to be 0.7–1.0%. The sidelobe structure is sketched using the analytical expression for diffraction efficiency from the Kogelnik theory,[7] matching the theory and the experiment on the Bragg angle only. The diffraction efficiency is given by

$$\eta = \sin^2[(\gamma^2 + \xi^2)^{1/2}]/(1 + \xi^2/\gamma^2), \quad (1)$$

where $\gamma = \pi n_1 d/[\lambda(c_R c_S)^{1/2}]$ is the modulation coefficient, $\xi = vd/(2c_S)$, n_1 is the amplitude of the sinusoidal

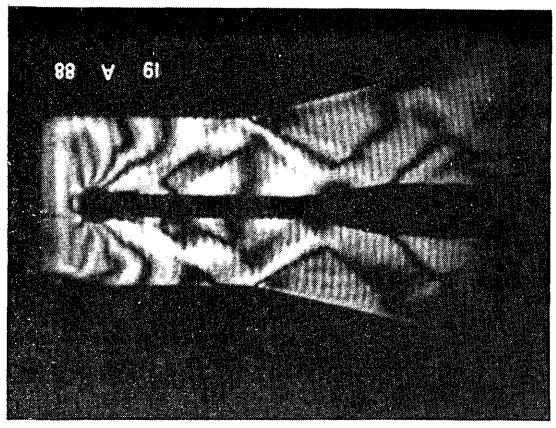

Fig. 5. Interferogram corresponding to the thirteenth angularly multiplexed double exposure hologram in a stack storing a sequence of flow field visualization results. The object is the same as that in Fig. 2, and the angular separation is $\Delta\theta' = 0.5°$.

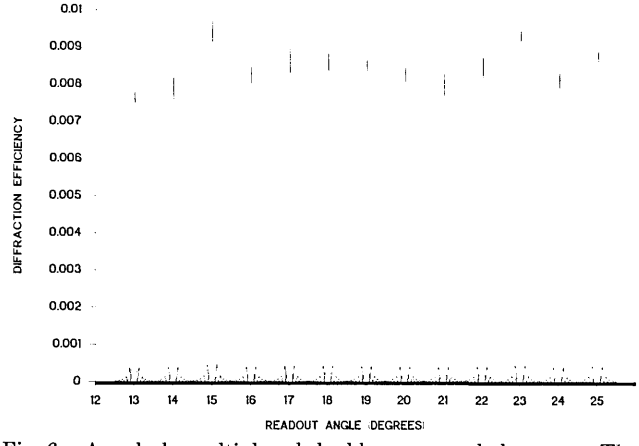

Fig. 6. Angularly multiplexed double exposure holograms. The diffraction efficiency vs the (external) readout angle is shown. The crystal thickness is 1.6 mm.

index modulation, d is the thickness of the crystal, λ is the free-space wavelength, $c_R = \cos\theta$ and $c_S = \cos\theta - \lambda\cos\phi/(n_0\Lambda)$ are the obliquity factors, v is the dephasing measure given by $v = \pi[2\cos(\phi - \theta) - \lambda/(n_0\Lambda)]/\Lambda$, n_0 is the bulk index of refraction, Λ is the grating spacing, ϕ is the slant angle, and θ is the internal readout angle. This is done to give an indication of the angular spread of the holograms in practice. In Fig. 7, it is indeed verified that the theory gives a reasonable estimate of the angular behavior. There, the angular selectivity of a single double exposure hologram with a Bragg angle of $\theta' = 15°$ is examined more carefully. Theory as represented by Eq. (1) and experiment are compared, matching the two at the Bragg angle. The theory intended to describe infinite plane wave readout of thick hologram gratings is seen to describe adequately the much more complicated situation of two superimposed Fourier transform data holograms, at least for the experimental conditions used here.

IV. Conclusions

Holographic interferometry using photorefractive crystals has been reported. Lithium niobate crystals

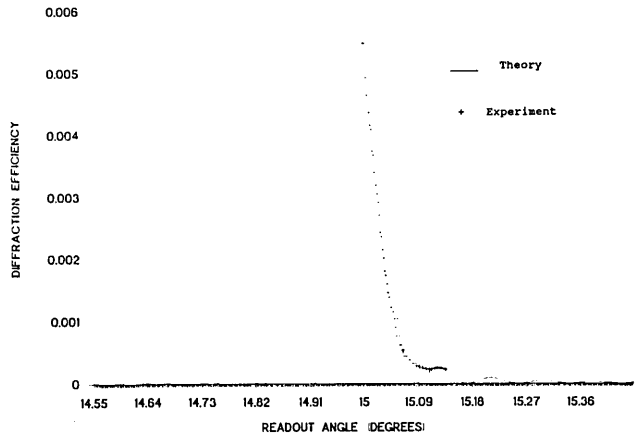

Fig. 7. Angular selectivity of a single double exposure hologram recorded in the crystal used in Fig. 6.

are well suited for this application. Simultaneous recording and storage of double exposure holograms is demonstrated via angular multiplexing. Angular packing density of more than two (double exposure) holograms per degree can be used with no crosstalk observed. The sensitivity of the technique used is also demonstrated. Changes in the aerodynamic conditions (pressure and object physical shape) produce clearly observable differences in the results. The resolution provided by the crystals is, therefore, ample for applications in aerodynamic flow field visualization.

This work was supported by the U.S. Army Research Office under grant DAA L03-86-K0149. The assistance of D. Shin in the laboratory is acknowledged.

References

1. A. M. Glass, "Photorefractive Effect," Opt. Eng. **17**, 470 (1978).
2. R. Magnusson, J. H. Mitchell III, T. D. Black, and D. R. Wilson, "Holographic Interferometry Using Iron-Doped Lithium Niobate," Appl. Phys. Lett. **51**, 81 (1987).
3. J. P. Huignard, and J. P. Herriau, "Real-Time Double-Exposure Interferometry with $Bi_{12}SiO_{20}$ Crystals in Transverse Electrooptic Configuration," Appl. Opt. **16**, 1807 (1977).
4. A. Marrakchi, J. P. Herriau, and J. P. Huignard, "Real-Time Holographic Interferometry with Photorefractive $Bi_{12}SiO_{20}$ Crystals," Proc. Soc. Photo-Opt. Instrum. Eng. **353**, 24 (1982).
5. J. P. Huignard, J. P. Herriau, and T. Valentin, "Time Average Holographic Interferometry with Photoconductive Electrooptic $Bi_{12}SiO_{20}$ Crystals," Appl. Opt. **16**, 2796 (1977).
6. Y. H. Ja, "Real-Time Double-Exposure Holographic Interferometry in Four-Wave Mixing with Photorefractive $Bi_{12}GeO_{20}$ Crystals," Appl. Opt. **21**, 3230 (1982).
7. H. Kogelnik, "Coupled Wave Theory for Thick Hologram Gratings," Bell Syst. Tech. J. **48**, 2909 (1969).